

Sequential phase transitions in thermoresponsive nanoemulsions

Lilian C. Hsiao^a and Patrick S. Doyle^{a,*}

^a Department of Chemical Engineering, Massachusetts Institute of Technology, MA, USA

* Corresponding author: pdoyle@mit.edu.

Supplementary Information and Figures

Temperature-dependent interdroplet bridging

A schematic of the proposed interdroplet bridging mechanism is shown in Supplementary Fig. S1. The PEGDA molecules contain hydrophobic functional endgroups that partition into the a PDMS droplet when the temperature is increased. The remaining free end can also partition into another droplet at the same time, resulting in attractive bridging. The range of the attraction is thus determined by the R_g of the PEGDA molecules.

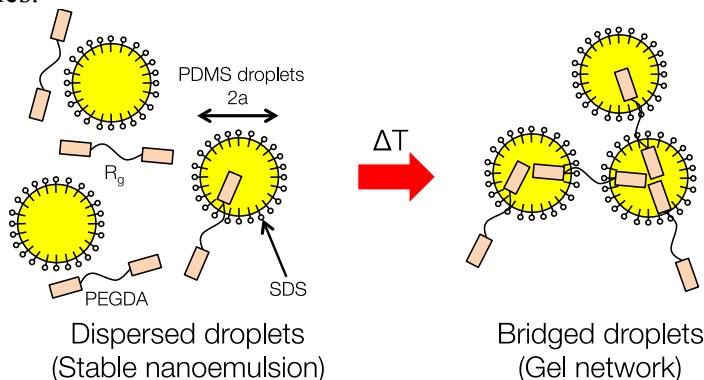


Figure S1. Schematic of temperature-driven interdroplet bridging of PEGDA between PDMS droplets. The two hydrophobic endgroups of the PEGDA are needed to bring droplets together as temperature is increased.

Effect of photoinitiator and dye on thermogelation

To ensure that the incorporation of the photoinitiator and lipophilic dye does not change thermogelling behavior, we systematically vary the concentration of both components and study the gel microstructure for nanoemulsions at $\phi = 0.25$. Supplementary Fig. S2 shows representative 2D CLSM images of gels at $T = 65^\circ\text{C}$ when the concentration of Darocur and PKH26 are independently varied between 0.25 vol% to 2 vol%. The $I(q)$ plots in Supplementary Fig. S3 show that the microstructure of the gels are quantitatively similar to one another (within experimental error). Temperature-ramp rheological measurements with pure nanoemulsions further show that the thermogelation is mostly unaffected by small quantities of the photoinitiator and the dye (Supplementary Fig. S4).

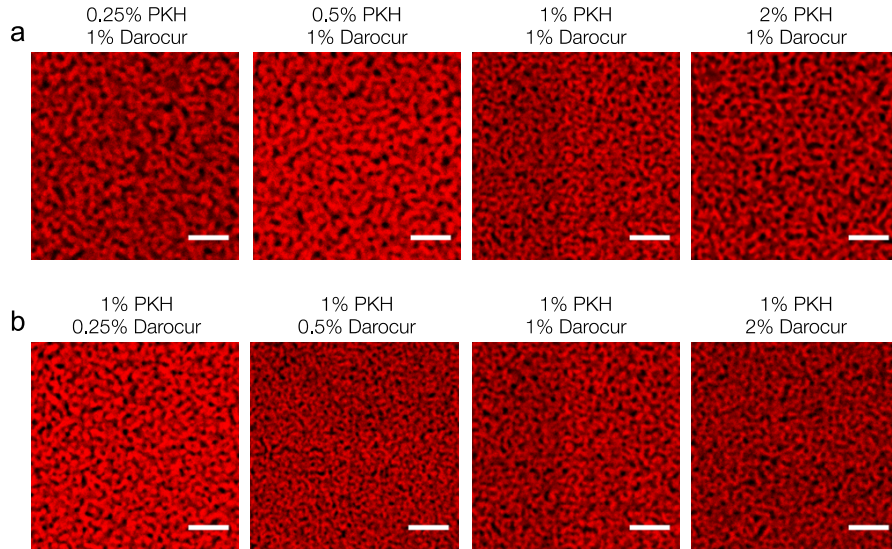


Figure S2. Effect of photoinitiator (Darocur) and dye (PKH26) on thermogelation. Representative 2D CLSM images of a nanoemulsion ($\phi = 0.25$) heated to $T = 65^\circ\text{C}$. Samples are locked in place prior to imaging. The effect on gel microstructure is studied for (a) varying PKH concentration with 1 vol% Darocur, and (b) varying Darocur concentration with 1 vol% PKH. Scale bars = 3 μm .

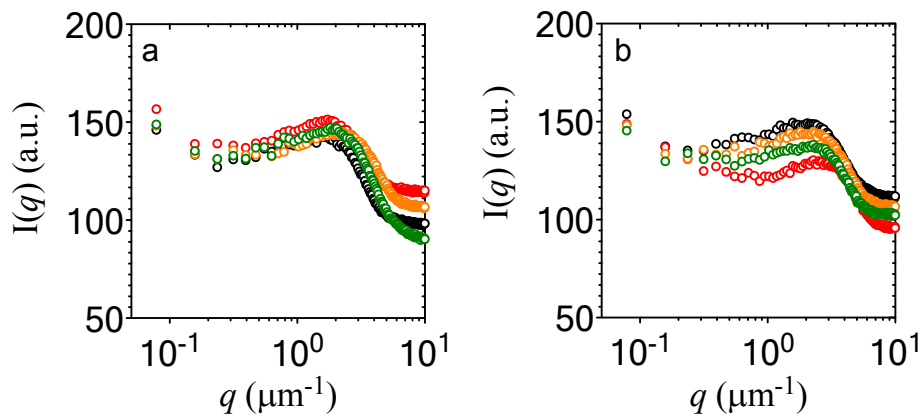


Figure S3. Quantification of gel microstructure with $I(q)$. These $I(q)$ plots are generated from the CLSM images presented in Fig. S2, where (a) represents gels with variable PKH concentration and 1 vol% Darocur, and (b) represents gels with variable Darocur concentration and 1 vol% PKH. The component with the varying composition is shown for 0.25 vol% (black), 0.5 vol% (red), 1 vol% (orange), and 2 vol% (green).

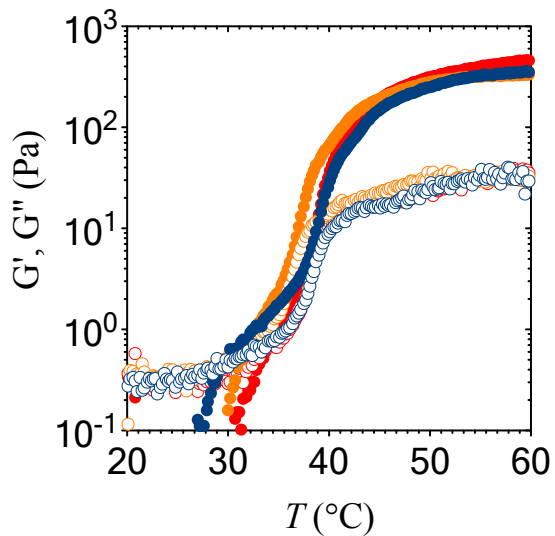


Figure S4. Effect of photoinitiator and dye on the temperature ramp oscillatory rheology. The thermogelling behavior of pure nanoemulsions (red), nanoemulsions with 1 vol% Darocur (orange), and nanoemulsions with 1 vol% Darocur and 1 vol% PKH26 (blue) are shown. Closed and open symbols represent G' and G'' respectively.

CLSM images of gels near the phase boundary

Close-up CLSM images of the gels show rich phase behavior close to the coexistence boundary. Examples are density fluctuations of the percolated structure, spinodal decomposition, and dynamical heterogeneity in which thick strands coexist with small clusters (Supplementary Fig. S5).

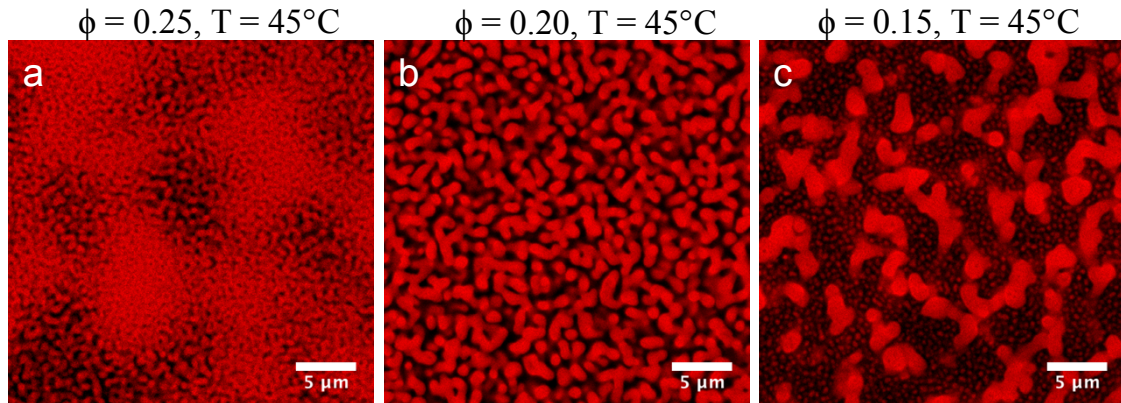


Figure S5. Representative 2D CLSM images of gels close to the phase boundary. Examples of gels with (a) density fluctuations, (b) spinodal decomposition, and (c) dynamical heterogeneity. Scale bars = 5 μ m.

Frequency-dependent small angle oscillatory rheology

We perform additional rheological characterization of the nanoemulsion at a specific volume fraction ($\phi = 0.33$), where we study the frequency-dependent response for a range of temperatures that spans the percolation and the phase separation regimes. The values of G' and G'' follow a power-law, $G' \sim \omega^m$ and $G'' \sim \omega^n$. When $m = 2$ and $n = 1$, the material is liquid-like; when $m \sim n \sim 0$, the material is solid-like [23]. Supplementary Fig. S6 shows that the nanoemulsions proceed from a liquid-like state at $T = 30^\circ\text{C}$ to solid-like states for $T \geq 40^\circ\text{C}$. At temperatures past the initial gel point ($T > 30^\circ\text{C}$), the only difference is the absolute magnitude of G' and G'' . That is, we show that both the percolated and the phase separated states are dynamically arrested, and that both types of microstructure can support a significant amount of elastic stress.

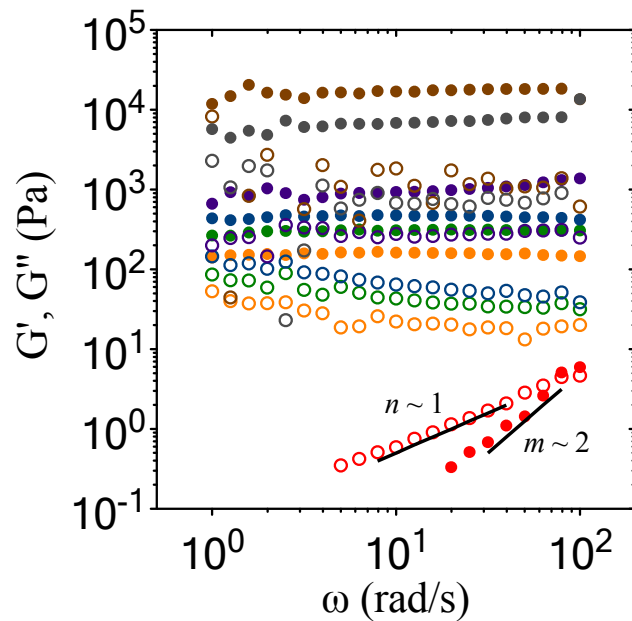


Figure S6. Frequency-dependent rheological characterization of nanoemulsions with $\phi = 0.33$. Data is shown for $T = 30^\circ\text{C}$ (red), 40°C (orange), 45°C (green), 50°C (blue), 55°C (purple), 60°C (brown), and 65°C (gray). Closed symbols are G' and open symbols are G'' .